CONFERENCE PRE-PRINT

NEUTRAL BEAM INJECTION FOR ELECTRON HEATING OF GLOBUS-M2 SPHERICAL TOKAMAK'S PLASMA

P.B. SHCHEGOLEV, <u>G.S. KURSKIEV</u>, N.S. ZHILTSOV, A.YU. TELNOVA, E.E. TKACHENKO, E.O. KISELEV, N.V. SAKHAROV, V.K. GUSEV, V.B. MINAEV, YU.V. PETROV, N.N. BAKHAREV, I.M. BALACHENKOV, V.I. VARFOLOMEEV, S.V. KRIKUNOV, A.K. KRYZHANOVSKII, A.D. MELNIK, I.V. MIROSHNIKOV, A.N. NOVOKHATSKII, M.I. PATROV, O.M. SKREKEL, V.V. SOLOKHA, N.V. TEPLOVA, V.A. TOKAREV, S.YU. TOLSTYAKOV, G.A. TROSHIN, E.A. TYUKHMENEVA, N.A. KHROMOV, F.V. CHERNYSHEV, K.D. SHULYATYEV

Ioffe Institute

St. Petersburg, Russia

Email: gleb.kurskiev@mail.ioffe.ru

A.A. KAVIN, A.B. MINEEV JSC "NIIEFA" St. Petersburg, Russia

A.M. PONOMARENKO, A.YU. YASHIN Peter the Great St. Petersburg Polytechnic University St. Petersburg, Russia

V.A. SOLOVEY

Petersburg Nuclear Physics Institute named by B.P. Konstantinov of NRC "Kurchatov Institute" St. Petersburg, Russia

E.G. ZHILIN Ioffe Fusion Technology Ltd. St. Petersburg, Russia

Abstract

The paper analyzes energy confinement of Globus-M2 spherical tokamak's plasma under a wide range of operating parameters (toroidal magnetic field up to 0.95 T, plasma current up to 0.45 MA) with neutral beam injection (beam power up to 1 MW, particle energy up to 50 keV). More than 300 deuterium plasma discharges with deuterium beam injection were analyzed. Linear regression indicates strong dependence of electron thermal energy and electron temperature on the plasma current and moderate dependence on the toroidal magnetic field. Thermal insulation of ions is much better than thermal insulation of electrons, and energy confinement time is determined primarily by plasma's electron component. Analysis of plasma stability in the gradient region showed that the development of electromagnetic instabilities is unlikely, while electrostatic electron temperature gradient mode is apparently unstable, and it determines electron heat transfer.

1. INTRODUCTION

Spherical tokamaks (STs), or tokamaks with a small aspect ratio A=R/a<2 (where **R** and **a** are major and minor radii, respectively), ensure stable operation with high plasma current at a relatively low toroidal magnetic field (B_T), reaching large toroidal beta $\beta_T \ge 30\%$ [1] and normalized beta $\beta_N \ge 6$ [2] values. While achieving high confinement mode (H-mode) regime, where ion heat transport remained at the neoclassical level [3], the first experiments on STs with $B_T \le 0.5$ T showed rather poor thermal insulation of the plasma with H-factor (the ratio of energy confinement time to predictions of widely used IPB98(y,2) scaling) of approximately 0.7 [4,5]. The main channel of heat loss was anomalous electron heat transport caused by micro-tearing (MTM) and electron temperature gradient (ETG) modes, and it rapidly decreased with decreasing collisionality [6-8], causing a strong dependence of energy confinement time on toroidal magnetic field in STs for B_T up to 0.8 T [9-11]. Independent investigations carried out on different STs have shown that energy confinement time (τ_E) exhibits strong dependence on B_T and moderate dependence on I_P [3].

However, there were reasonable doubts concerning the achievability of good confinement in STs at low collisionality $v^* \infty n/T^2$ expected for operational regimes with high B_T . For such conditions, M. Valovič, R. Akers,

M. de Bock et al. suggested the development of ion temperature gradient mode (ITG) that drives high ion heat fluxes [9]. Moreover, on NSTX for regimes with low electron collisionality v_e^* <0.15, strong enhancement of ion heat transport above the neoclassical level was observed [10] in discharges with B_T =0.55 T. First experiments on plasma heating that used neutral beam in Globus-M2 at B_T =0.8 T and collisionality <0.015 also demonstrated poor ion heating due to the development of the ITG mode. Nevertheless, later experiments on Globus-M2 (B_T =0.9) and ST40 (B_T =1.9) tokamaks achieved hot ion mode with fusion-relevant ion temperatures of 4 and 9 keV, respectively, using similar plasma heating scenarios with two neutral beams [12,13]. The obtained result shows some promise regarding ambitious projects based on STs using D-T reaction (STEP project [14]), p-B¹¹ fusion (EHL-2 [15] project) and a prototype of a fusion neutron source for rector materials testing [16]. The design of any of these devices requires reliable predictions of expected plasma parameters far beyond the explored area. The only way to solve this problem is to consistently build experimental setups with parameters approaching target values.

This paper reviews main energy confinement features of ST plasmas heated by neutral beams in a wide range of B_T =0.5-0.9 T discovered in the Globus-M2. Section 2 of the paper describes the experiment setup; Section 3 discusses the criteria for forming a representative sample of discharges for analysis; Section 4 is devoted to plasma energy confinement; and Section 5 analyzes the stability of discharges to the development of turbulence modes. The Discussion and Conclusions section sums up the main results.

2. EXPERIMENT SETUP

Experiments were carried out on Globus-M2 spherical tokamak [17] using a wide range of plasma current (I_p) from 0.15 to 0.45 MA, toroidal magnetic field (B_T) from 0.5 to 0.95 T, and electron plasma density (n_e) from 1 to 9 10⁻¹⁹m⁻³. Tokamak plasma had a divertor configuration with elongation up to 1.8 and triangularity up to 0.35. Neutral beam injector NBI-2 [17] created a beam of high-energy deuterium atoms with power (P_b) from 0.25 to 1.00 MW and no more than 11 cm in diameter (at 1/e power level). Neutral injection was performed in the equatorial plane of the torus in tangential direction along the plasma current; the impact parameter was 30 cm. The discharge scenario included: a stage of plasma current rise, whereat the atomic beam started to be injected; transition to a quasi-stationary phase on the current plateau, whereat it was maintained at a constant level according to a predetermined program; and the end of the discharge synchronized with the cessation of neutral injection. Active charge exchange spectroscopy (CXRS) diagnostics allowed to measure the ion temperature (T_i) . Thomson scattering (TS) diagnostic was used to measure electron density (n_e) and electron temperature (T_e) spatial distributions at 11 spatial points located from the magnetic axis to the plasma boundary on the low-field side every 3.03 ms. The shape of the last closed magnetic surface of the plasma column was reconstructed using the algorithm of moving current filaments [19] and the pyGSS code [20]. ASTRA transport code [21] was used for heat transport analysis and calculation of the ohmic heating power. Calculations of the NBI heating power for electrons and ions were performed using a modified orbital code developed specifically for the conditions of Globus-M2 tokamak [22] and the NUBEAM code [23].

3. DATA SELECTION

A representative dataset was formed from an extensive tokamak database and used it to analyze heat transport of Globus-M2 tokamak plasma's electrons and ions in NBI discharges. In these discharges, only one deuterium beam of the NBI-2 was used. The plasma was also deuterium. The authors relied on a quasi-stationary phase of the discharges with no large-scale MHD disturbances, such as the Internal Reconnection Event (IRE). The time interval was selected starting 10 ms after the plasma current reached a plateau until the end of the discharge, and the duration of such an interval should be at least 20 ms. Discharges with locked MHD were also filtered, and the presence of the locked mode was determined in accordance with the approach developed in [24]. As a result, the representative dataset consisted of over 300 discharges, comprising more than four thousand profiles of electron temperature and density. Measured central electron temperature (T_e^0) vs respective central electron density (T_e^0) in discharges with different T_e^0 0 has a magnitude of plasma holding magnetic field on its electron temperature, which reaches 1.8 keV. At the same time, central ion temperature (T_e^0 1) was as high as 2.9 keV (T_e^0 1), and plasma was in hot ion mode, which was previously achieved only by using two neutral beams simultaneously [13].

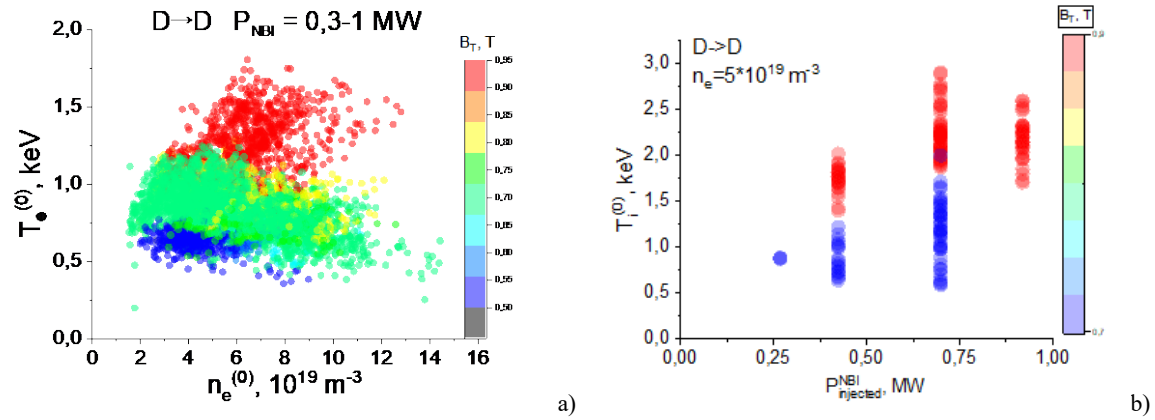


FIG. 1. (a) Dependence of core electron temperature on core density and toroidal magnetic field in Globus-M2 NBI heated plasma. (b) Dependence of core ion temperature on NBI heating power and toroidal magnetic field for discharges with average plasma density $5 \cdot 10^{19}$ m⁻³.

4. IMPACT OF PLASMA CURRENT AND TOROIDAL MAGNETIC FIELD ON ENERGY CONFINEMENT

Analysis of TS diagnostic data along with magnetic equilibrium reconstruction results allowed for determining electron stored thermal energy (W_e) . It should be noted that, for all the discharges in the dataset, total stored plasma energy W_{MHD} is more than double the value of W_e , as shown in FIG. 2a. This indicates a noticeable excess of ion temperature over plasma electron temperature, which is confirmed by the CXRS data. Plasma current (I_p) , toroidal magnetic field (B_T) , average electron density (n_e) , and the power of the atomic beam (P_{NBI}) were chosen as the main parameters influencing the efficiency of plasma heating. Linear regression of data indicates a strong dependence of W_e and T_e on plasma or a moderate dependence on the toroidal magnetic field $W_e \sim I_p^{1.07} B_T^{0.6} n_e^{0.63} P_{NBI}^{0.08}$; $\langle T_e \rangle_V \sim I_p^{0.95} B_T^{0.54} n_e^{-0.25} P_{NBI}^{0.06}$. The results of regression analysis are presented in FIG. 2b,c. The effect of injected beam power on

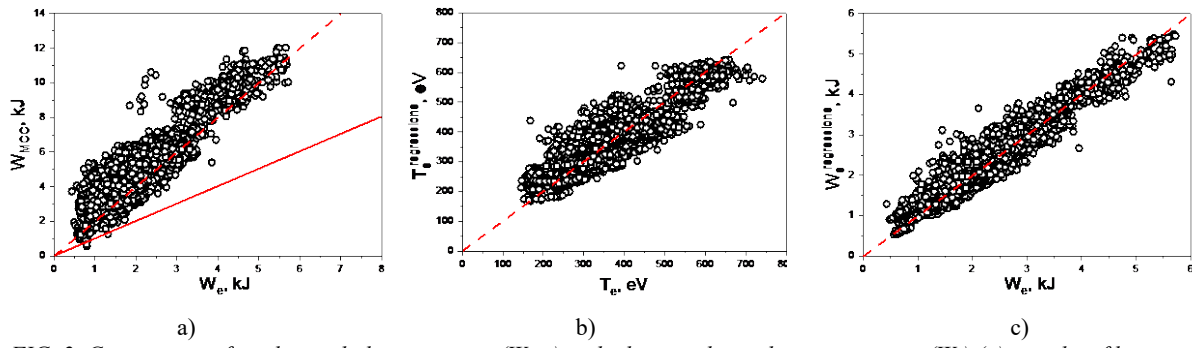


FIG. 2. Comparison of total stored plasma energy (W_{mcc}) with electron thermal energy content (W_e) (a); results of linear regression of electron temperature (b); and electron thermal energy content (c) with the corresponding experimentally measured values.

electron temperature and, consequently, on energy stored in the electron component of plasma is negligibly small. To clarify the reasons behind such results, we analyzed two cases for fixed $n_e = 5 \cdot 10^{-19} \text{ m}^{-3}$ (that corresponds to maximum ion temperatures): $I_p = 300 \text{ kA}$, $B_T = 0.7 \text{ T}$ and $I_p = 400 \text{ kA}$, $B_T = 0.9 \text{ T}$ for P_{NBI} values varying by a factor of 3. For clarity, FIG. 3a shows electron plasma temperature profiles for discharges with fixed $B_T = 0.9 \text{ T}$, $I_p = 400 \text{ kA}$ and variable atomic beam power of 425, 700 and 925 kW. They are identical, while T_e profiles for discharges with different I_p and B_T ($I_p = 300 \text{ kA}$, $B_T = 0.7 \text{ T}$ vs $I_p = 400 \text{ kA}$, $B_T = 0.9 \text{ T}$) with fixed moderate P_{NBI} (b) differ by a factor of two, see FIG. 3b. Estimated electron heating powers for these cases are shown in FIG. 4.

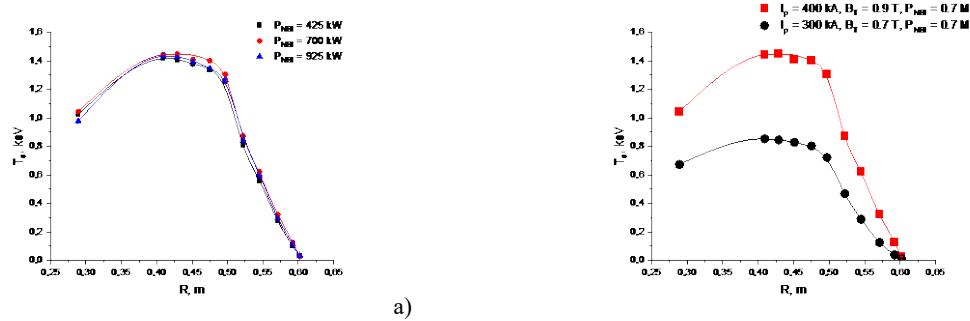


FIG. 3. Electron temperature profiles for discharges with $I_p = 400 \text{ kA}$, $B_T = 0.9 \text{ T}$ for variable atomic beam power of 425, 700 and 925 kW (a); and comparison of T_e profiles for discharges with fixed NBI power of 0.7 MW and different I_p and B_T : $I_p = 300 \text{ kA}$, $B_T = 0.7 \text{ T}$ and $I_p = 400 \text{ kA}$, $B_T = 0.9 \text{ T}$ (b)

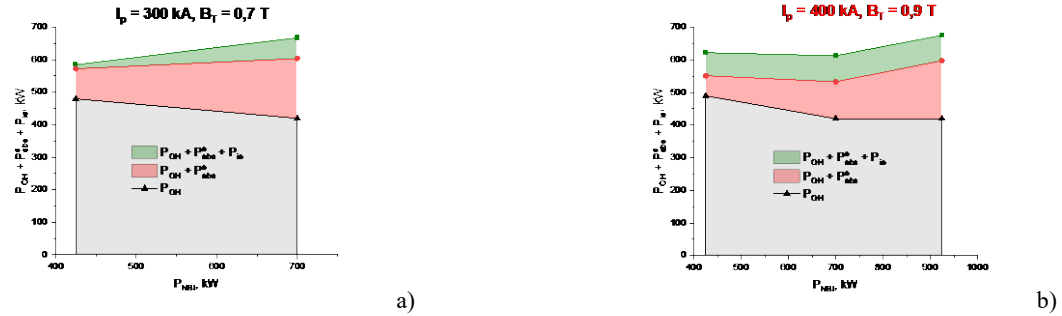


FIG. 4. Resulting electron heating power including beam, ohmic and electron-ion heat exchange vs NBI power for cases with $I_p = 300$ kA, $B_T = 0.7$ T (a) and $I_p = 400$ kA, $B_T = 0.9$ T (b)

FIG. 4 can see that the main source of plasma electron heating is the ohmic power. The increase in the total heating power of plasma electron component with increasing P_{NBI} is less than 10% due to the simultaneous decrease in P_{OH} . The decrease in the ohmic power is associated with higher neutral beam current drive, which partially replaces the plasma current. It should be noted that the ohmic heating power remains at the same level for cases (a) and (b) in FIG. 4 in spite of higher plasma current due to higher electron temperature (see FIG. 3b). Electron energy confinement time τ^e_E is shown in FIG. 5a. With an increase in the plasma current from 300 to 400 kA and the magnetic field from 0.7 to 0.9 T, τ^e_E increases by a factor of 1.6 (from 4.3 to 7 ms).

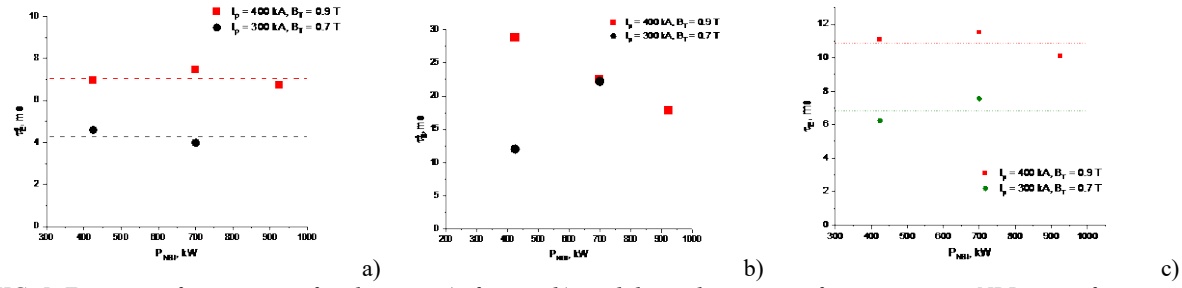


FIG. 5. Energy confinement time for electrons a); for ions b); and thermal energy confinement time vs NBI power for cases with $I_p = 300 \text{ kA}$, $B_T = 0.7 \text{ T}$ and $I_p = 400 \text{ kA}$, $B_T = 0.9 \text{ T}$ c)

FIG. 6 shows averaged measured T_i profiles for the aforementioned groups of discharges. A 1.3-fold increase in B_T and I_p at a fixed P_{NBI} leads to a twofold increase in ion temperature and a stable hot ion mode. However, maximum T_i achieved when operating with a single NBI is significantly lower than when operating using two heating beams [13].

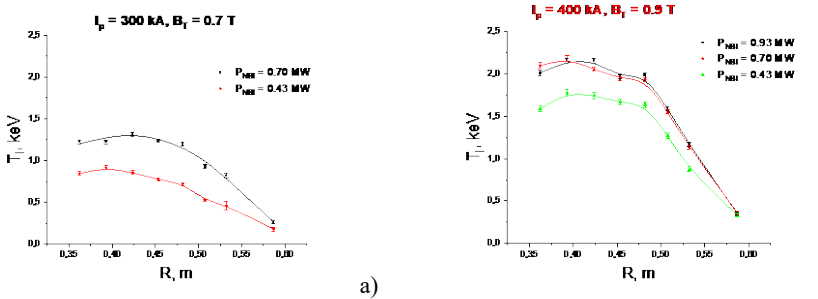


FIG. 6. Measured ion temperature profiles for cases with Ip = 300 kA, $B_T = 0.7 \text{ T}$ for NBI power of 280, 430 and 700 kW (a); and for discharges with $I_P = 400 \text{ kA}$, $B_T = 0.9 \text{ T}$ at P_{NBI} of 430, 700 and 930 kW (b)

b)

Ion heating powers are shown in FIG. 7 for the respective discharges. The main source of ion heating in these discharges is neutral beam injection. Due to an increase in the input beam power, the total power of ion heating increases significantly. As a result, the ion temperature in these discharges exceeds the electron temperature. As a result, ion cooling by electron-ion collisions is as high as 20-30% of the beam power absorbed by ions (P_i^{abs}) .

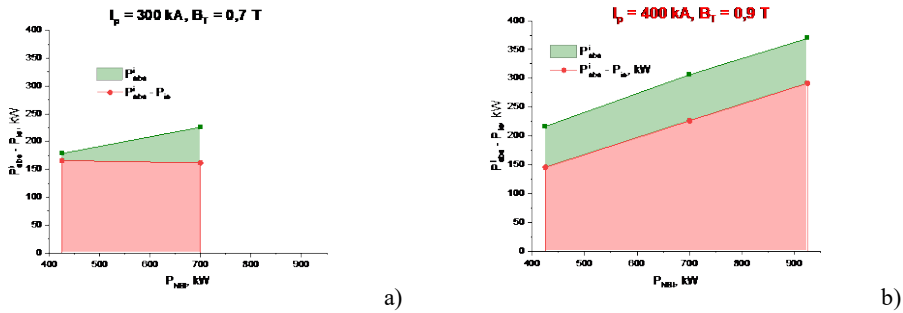


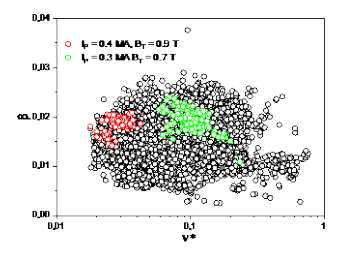
FIG. 7. Resulting ion heating power including the power electron-ion heat exchange vs atomic beam power for discharges with $I_p = 300 \text{ kA}$, $B_T = 0.7 \text{ T}$ (a) and $I_p = 400 \text{ kA}$, $B_T = 0.9 \text{ T}$ (b)

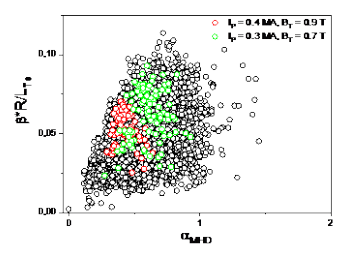
Ion energy confinement time τ_E^i , is shown in FIG. 5b. Thermal insulation of ions is significantly better than thermal insulation of electrons (τ_E^i is 2.5-4 times higher than τ_E^e). For I_p =400 kA and B_T = 0.9 T, τ_E^i decreases monotonically with increasing ion heating power. For I_p = 300 kA and B_T = 0.7 T, the τ_E^i trend is the opposite. At P_{NBI} =700 kW, the values of ion energy confinement time are the same for I_p = 400 kA, B_T = 0.9 T and I_p = 300 kA, B_T = 0.7 T, i.e., there is no dependence on the plasma current and magnetic field, even though, according to the neoclassical theory, τ_E^i should increase with increasing I_p and I_p . The reasons behind this result are unclear and warrant a separate study.

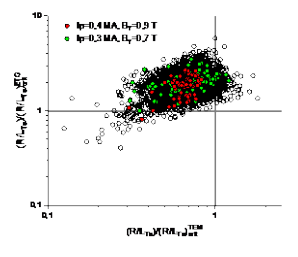
Analysis of plasma energy confinement was performed for fixed $n_e = 5 \cdot 10^{-19} \text{ m}^{-3}$, whereat maximum ion temperature values were achieved. Results are presented in FIG. 5c for $I_p = 400 \text{ kA}$, $B_T = 0.9 \text{ T}$ and $I_p = 300 \text{ kA}$, $B_T = 0.7 \text{ T}$ vs the NBI power. An increase in B_T and I_p by a factor of 1.3 leads to a more than 1.4-fold increase in τ_E , which supports the predictions of scalings obtained earlier at the Globus-M2 tokamak [11]. According to ST-like scalings $\tau_E^{Globus-21} \sim I_p^{0.53} \cdot B_T^{1.05}$ and $\tau_E^{GLB_2020} \sim I_p^{0.43} \cdot B_T^{1.19}$ the enhancement in energy confinement time should reach 1.5, while for the IBP98(y,2) scaling $\tau_E^{IPB98(y,2)} \sim I_p^{0.93} \cdot B_T^{0.15}$ it should be 1.3. The increase in τ_E is mostly due to the decrease of electron heat transport, i.e., thermal insulation of electrons determines plasma's global thermal energy confinement.

5. ANALYSIS OF MICROINSTABILITIES

To analyse the stability of plasma to the development turbulent modes affecting electron heat transfer, the local dimensionless parameters were estimated for gradient region of the plasma r/a \approx 0.7: $\beta_e = 8\pi n_e T_e/B_T^2$, collisionality $\nu^* \approx 0.1 \frac{n_e^* Z_{eff}}{T_e^2}$; $L_T = -[\partial (\ln T)/r]^{-1}$ and the parameter $\alpha_{mhd} = -q^2 R d\beta/dr$, see FIG. 9







c)

b)

FIG. 8 Dimensionless parameter space: β_e vs v^* (a); product of β_e and R/L_{Te} vs α_{mhd} (b); comparison of R/L_{Te} with threshold values for TEM and ETG (c) discharges with average electron density $5 \cdot 10^{-19}$ m⁻³. Red dots stand for discharges with I_p =0.4 MA, B_T =0.9 T; green dots stand for discharges with I_p = 0.3 MA, B_T =0.7 T.

According to simulations carried out for the NSTX spherical tokamak [25], the following conditions should be met for the development of micro-tearing instability: $\beta_e > 4\%$ and $\beta_e R/L_{Te} > 10\%$. For the kinetic ballooning mode, normalized plasma pressure should be even higher: $\beta_e > 5-10\%$ and $\alpha_{mhd} \sim 1$. FIG. 8a,b shows that for the discharges under consideration maximum values of β_e are below 3%; therefore, the development of electromagnetic instabilities is highly unlikely. However, electrostatic trapped electron mode (TEM) or electrontemperature-gradient mode (ETG) can lead to significant heat transfer in the electron channel. A prerequisite for their development is that R/L_{Te} exceeds the threshold value.

The authors used the following thresholds for TEM [26]:
$$\frac{R^{TEM}}{L_{T_{e,crit}}} = \frac{0.357\sqrt{\epsilon} + 0.271}{\sqrt{\epsilon}} \left[4.90 - 1.31 \frac{R}{L_N} + 2.68 \hat{s} + \ln(1 + 20\nu^*) \right]$$
 and ETG [27]
$$\frac{R^{ETG}}{L_{T_{e,crit}}} = \left(1 + Z_{eff} \frac{T_e}{T_i} \right) \left(1.33 + 1.91 \frac{\hat{s}}{q} \right) f(\epsilon).$$

The comparison of estimated R/L_{Te} with threshold values is shown in FIG. 8c. Threshold values of ETG instability development are significantly lower than the ones observed in the experiment. Earlier GENE [28] simulations for the Globus-M2 tokamak plasma almost always demonstrated significant increments for the ETG. At the same time, threshold values for the TEM instability development are higher than those observed experimentally. Therefore, TEM instability seems to be stable. As a result, we can conclude that the electrostatic ETG instability is probably unstable and determines electron transport in the considered regime. In the NSTX spherical tokamak in discharges with a moderate value of the β_e parameter (less than 5%), thermal insulation of electrons was determined exactly by this instability [29-31], which resulted in improved thermal insulation of electrons while reducing plasma collisionality.

DISCUSSION AND CONCLUSIONS

Linear regression of experimental data indicates a strong dependence of W_e and T_e on the plasma current and a moderate dependence on the toroidal magnetic field, while the effect of injected beam power is negligible. With an increase in the injected beam power, electron temperature does not increase because the resulting electron heating power does not rise. An increase in I_{ν} and B_T leads to an increase in the electron temperature due to improved thermal insulation of electrons. Comparative analysis of the energy balance shows that, with a 1.3-fold increase in B_T and I_p and I_{NBI} , energy confinement time increases by 60%, which is consistent with the predictions of previously obtained scalings for spherical tokamaks. Thermal insulation of ions is much better than that of electrons, and τ_E is determined primarily by plasma's electron component. Analysis of plasma stability in the gradient zone r/a=0.7 shows that the development of electromagnetic instabilities, such as MTM and KBM, is unlikely due to low values of β_e <3%, while electrostatic ETG is apparently unstable, and it likely determines electron heat transfer in the considered regimes.

On compact spherical tokamak Globus-M2 with $B_T \ge 0.7$ T and neutral beam heating, hot ion mode appears to be a natural operating regime. On Globus-M2, hot ion mode was successfully achieved even with sawtooth oscillations. Hot ion mode was also achieved on the ST40 tokamak at toroidal magnetic fields of $B_T = 1.7-2$ T [32,33]. FIG. 9a presents a comparison of the H-factor versus B_T and average heat diffusivity versus effective collisionality, and combines data from Globus-M2 and ST40. On Globus-M2, thermal confinement improves significantly with an increase in toroidal magnetic field. However, this trend saturates at an H-factor (the ratio of energy confinement time to predictions of IPB98(y,2) scaling) of ~1.4, indicating a limit to confinement enhancement in spherical tokamaks with further B_T increase. Despite a twofold difference in the toroidal magnetic field between ST40 and Globus-M2, the values of ion and electron heat diffusivities are similar (see FIG. 9b). This further supports the scaling saturation hypothesis and emphasizes that predictive modeling with scalings of plasma parameters for future spherical tokamaks should be approached with caution. Such simulations should be based on first-principles physics-based models.

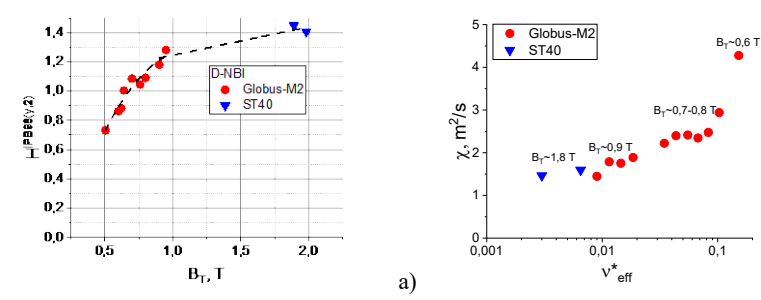


FIG. 93. (a) Dependence of H-factor on toroidal magnetic field for Globus-M2 and ST40 data [33]; (b) average heat diffusivity vs collisionality for Globus-M2 and ST40 data [33].

ACKNOWLEDGEMENTS

b)

The experiments were carried out at the Unique Scientific Facility "Spherical Tokamak Globus-M," which is incorporated in the Federal Joint Research Center "Material science and characterization in advanced technology." Plasma heating experiments with NBI presented in Section "Experiment setup" were financially supported by the FFUG-2021-0001 project. Measurements of electron temperature and density spatial distributions (Section "Data selection") were financially supported by the FFUG-2024-0028 project. The energy confinement study (Sections "Impact of plasma current and toroidal magnetic field on energy confinement", "Analysis of microinstabilities" and "Discussion and conclusions") was carried out with the financial support of the Russian Science Foundation, project No. 24-12-00162.

REFERENCES

- M. Gryaznevich, R. Akers, P. G. Carolan et al. "Achievement of Record b in the START Spherical Tokamak" Phys. Rev. Lett., 1988, 80, 3972 DOI: https://doi.org/10.1103/PhysRevLett.80.3972
- 2. J.E. Menard, M.G. Bell, R.E. Bell et al. "β-Limiting MHD instabilities in improved-performance NSTX spherical torus plasmas" Nucl. Fusion 43 (2003) 330–340 DOI 10.1088/0029-5515/43/5/305
- 3. S M Kaye, J W Connor and C M Roach "Thermal confinement and transport in spherical tokamaks: a review" 2021 Plasma Phys. Control. Fusion 63 123001DOI 10.1088/1361-6587/ac2b38
- 4. S.M. Kaye, M.G. Bell, R.E. Bell et al. "Energy confinement scaling in the low aspect ratio National Spherical Torus Experiment (NSTX)" 2006 Nucl. Fusion 46 848 DOI 10.1088/0029-5515/46/10/002
- R J Akers, J W Ahn, G Y Antar et al. "Transport and confinement in the Mega Ampère Spherical Tokamak (MAST) plasma" 2003 Plasma Phys. Control. Fusion 45 A175 DOI 10.1088/0741-3335/45/12A/013
- W. Guttenfelder, J. Candy, S. M. Kaye et al. "Electromagnetic Transport from Microtearing Mode Turbulence" Phys. Rev. Lett. 106, 155004 DOI: https://doi.org/10.1103/PhysRevLett.106.155004
- E. Mazzucato, D. R. Smith, R. E. Bell et al. "Short-Scale Turbulent Fluctuations Driven by the Electron-Temperature Gradient in the National Spherical Torus Experiment" Phys. Rev. Lett. 101, 075001 DOI: https://doi.org/10.1103/PhysRevLett.101.075001
- 8. Y. Ren, S. M. Kaye, E. Mazzucato et al. "Density Gradient Stabilization of Electron Temperature Gradient Driven Turbulence in a Spherical Tokamak" Phys. Rev. Lett. 106, DOI: https://doi.org/10.1103/PhysRevLett.106.165005
- M. Valovič, R. Akers, M. de Bock et al. "Collisionality and safety factor scalings of H-mode energy transport in the MAST spherical tokamak" 2011 Nucl. Fusion 51 073045 DOI 10.1088/0029-5515/51/7/073045
- S.M. Kaye, S. Gerhardt, W. Guttenfelder et al. "The dependence of H-mode energy confinement and transport on collisionality in NSTX" 2013 Nucl. Fusion 53 063005 DOI 10.1088/0029-5515/53/6/063005
- 11. G.S. Kurskiev, V.K. Gusev, N.V. Sakharov et al. "Energy confinement in the spherical tokamak Globus-M2 with a toroidal magnetic field reaching 0.8 T" G.S. Kurskiev et al 2022 Nucl. Fusion 62 016011 DOI 10.1088/1741-4326/ac38c9
- 12. G.S. Kurskiev, I.V. Miroshnikov, N.V. Sakharov et al. "The first observation of the hot ion mode at the Globus-M2 spherical tokamak" 2022 Nucl. Fusion 62 104002 DOI 10.1088/1741-4326/ac881d

- 13. G. S. Kurskiev, V. B. Minaev, N. V. Sakharov et al. "Confinement, heating, and current drive study in Globus-M2 toward a future step of spherical tokamak program in Ioffe Institute" Phys. Plasmas 31, 062511 (2024) https://doi.org/10.1063/5.0211866
- H. Anand, O. Bardsley, D. Humphreys et al. "Modelling, design and simulation of plasma magnetic control for the Spherical Tokamak for Energy Production (STEP)" Fusion Engineering and Design, Volume 194, September 2023, 113724 https://doi.org/10.1016/j.fusengdes.2023.113724
- 15. Yunfeng LIANG, Huasheng XIE, Yuejiang SHI et al. "Overview of the physics design of the EHL-2 spherical torus" 2025 Plasma Sci. Technol. 27 024001 DOI 10.1088/2058-6272/ad981a
- 16. V. B. Minaev, A. B. Mineev, N. V. Sakharov et al. "Development of Next-Generation Spherical Tokamak Concept. The Globus-3 Tokamak" Plasma Phys. Rep. 49, 1578–1587 (2023). https://doi.org/10.1134/S1063780X23601189
- P.B. Shchegolev, V.B. Minaev, A.Y. Telnova et al. Neutral Injection Complex for Globus-M2 Spherical Tokamak. Plasma Phys. Rep. 49, 1501–1514 (2023). https://doi.org/10.1134/S1063780X23601098
- 18. Yu.V. Petrov et al, 2024 Plasma Physics Reports, Vol. 49, pp. 1459-1479
- V.I. Vasiliev, Yu.A. Kostsov, K.M. Lobanov, L.P. Makarova, A.B. Mineev, V.K. Gusev, R.G. Levin, Yu.V. Petrov, N.V. Sakharov // Nucl. Fusion. V. 46. P. S625 (2006) doi:10.1088/0029-5515/46/8/S08
- E. O. Kiselev, I. M. Balachenkov, N. N. Bakharev, V. I. Varfolomeev, V. K. Gusev, N. S. Zhiltsov, O. A. Zenkova, A. A. Kavin, G. S. Kurskiev, V. B. Minaev, I. V. Miroshnikov, M. I. Patrov, Yu. V. Petrov, N. V. Sakharov, O. M. Skrekel, V. V. Solokha, A. Yu. Telnova, E. E. Tkachenko, V. A. Tokarev, E. A. Tukhmeneva, N. A. Khromov, P. B. Shchegolev // Plasma Phys. Rep., 2023, v.49, 12, pp. 1560-1577, https://doi.org/10.1134/S1063780X23601621
- 21. G. Pereverzev, P.N. Yushmanov, Max-Plank IPP report 5/98 (2002)
- Bakharev N.N., Chernyshev F.V., Goncharov P.R., Gusev V.K., Iblyaminova A.D., Kornev V.A., Kurskiev G.S., Melnik A.D., Minaev V.B., Mironov M.I., Patrov M.I., Petrov Yu.V., Sakharov N.V., Shchegolev P.B., Tolstyakov S.Y., Zadvitskiy G.V. // Nucl. Fusion. IOP Publishing, 2015. Vol. 55, No. 4. P. 43023. doi: 10.1088/0029-5515/55/4/043023
- 23. A. Pankin et al., The tokamak Monte Carlo fast ion module NUBEAM in the National Transport Code Collaboration library, Computer Physics Communications 159 (2004) 157–184, doi:10.1016/j.cpc.2003.11.002.
- 24. Yu. V. Petrov, I. M. Balachenkov, N. N. Bakharev, V. I. Varfolomeev, A. V. Voronin, V. K. Gusev, N. S. Zhiltsov, A. A. Kavin, E. O. Kiselev, G. S. Kurskiev, V. B. Minaev, I. V. Miroshnikov, A. N. Novokhatskii, N. V. Sakharnov, O. M. Skrekel, V. V. Solokha, A. Yu. Telnova, E. E. Tkachenko, V. A. Tokarev, S. Yu. Tolstyakov, E. A. Tukhmeneva, N. A. Khromov, P. B. Shchegolev, K. D. Shulyatyev // Plasma Phys. Rep., 2024, Vol. 50, pp. 773–780, https://doi.org/10.1134/S1063780X24600932
- 25. Guttenfelder // Nucl. Fusion 53 (2013)
- 26. A. G. Peeters, C. Angioni, M. Apostoliceanu, F. Jenko, F. Ryter, the ASDEX Upgrade team// Phys. Plasmas 12, 022505 (2005), https://doi.org/10.1063/1.1848111
- 27. F. Jenko, W. Dorland // Phys. Rev. Lett., 2002, 89. 225001, https://doi.org/10.1103/PhysRevLett.89.225001
- 28. T. Dannert, F. Jenko // Phys. Plasmas, 2005, Vol. 12. 072309, https://doi.org/10.1063/1.1947447
- 29. Ghim Y.C. et al 2014 Nucl. Fusion 54 042003
- 30. Ghim Y.C. et al 2013 Phys. Rev. Lett. 110 145002
- 31. Guttenfelder W., Kaye S.M., Ren Y., Solomon W., Bell R.E., Candy J., Gerhardt S.P., LeBlanc B.P. and Yuh H. 2016 Phys. Plasmas 23 052508
- S.A.M. McNamara, O. Asunta, J. Bland et al. "Achievement of ion temperatures in excess of 100 million degrees Kelvin in the compact high-field spherical tokamak ST40" 2023 Nucl. Fusion 63 054002 DOI 10.1088/1741-4326/acbec8
- 33. S M Kaye, M Sertoli, P Buxton et al. "Isotope dependence of transport in ST40 hot ion mode plasmas" 2023 Plasma Phys. Control. Fusion 65 095012 DOI 10.1088/1361-6587/ace849